The Preparation, Characterization, and Magnetism of Copper 15-Metallacrown-5 Lanthanide Complexes

Ann J. Stemmler,[†] Jeff W. Kampf,[†] Martin L. Kirk,[‡] Bassel H. Atasi,[†] and Vincent L. Pecoraro*,[†]

Department of Chemistry, The University of Michigan, Ann Arbor, Michigan 48109-1055, and Department of Chemistry, The University of New Mexico, Albuquerque, New Mexico 87131-1096

Received January 7, 1998

The preparation and characterization of a series of encapsulated-lanthanide 15-metallacrown-5 complexes are reported. Planar ligands such as picoline hydroxamic acid (picha) or nonplanar α-amino hydroxamic acids (e.g., glycine hydroxamic acid (glyha)) led to one-step syntheses of metallacrowns in yields as high as 85%. The reaction of the appropriate hydroxamic acid with copper acetate and $^1/_5$ equiv of gadolinium(III) or europium(III) nitrates in DMF or water yielded crystals of $Gd(NO_3)_3$[15-$MC_{Cu(II)N(picha)}$-5], **1**, $Eu(NO_3)_3$[15-$MC_{Cu(II)N(picha)}$-5], **2**, and $Eu(NO_3)_3$[15-$MC_{Cu(II)N(glyha)}$-5], **3**. Several other 15-metallacrown-5 complexes were synthesized with (1) Cu(II) or Ni(II) in the metallacrown ring metal position, (2) various lanthanides (La(III), Nd(III), Sm(III), Eu(III), Gd(III), Dy(III), Ho(III), Er(III), and Yb(III)) encapsulated in the center of the ring, and (3) chiral α-amino hydroxamic acids (e.g., phenylalanine hydroxamic acid (H_2pheha), leucine hydroxamic acid (H_2leuha), and tyrosine hydroxamic acid (H_2tyrha)). It is believed that all of the complexes containing Cu(II) ions have the ring metals either in four-coordinate, square-planar environments, bound to two tetradentate hydroximate ligands, or in five-coordinate, square-pyramidal geometries if solvent is bound. Spectroscopic and magnetic characterization of the Ni(II) complexes suggests that they are either five- or six-coordinate. The encapsulated lanthanides are generally pentagonal bipyramidal, with five oxygen donors from the metallacrown ring and solvent or bidentate nitrate ions in the axial positions. The circular arrangement of ions results in interesting magnetic behavior. With Dy(III) encapsulated in the center of the ring, a magnetic moment as high as 10.9 μ_B is achieved. Analysis of the variable-temperature susceptibility of $La(NO_3)_3$[15-$MC_{Cu(II)N(picha)}$-5] indicates that the five Cu(II) ions are antiferromagnetically coupled, forming an $S = {}^1/_2$ ground spin state with a moment of 1.7 μ_B at liquid helium temperatures. Complex **1** shows ferromagnetic coupling of the Gd(III) ion to the five Cu ions at temperatures below 15 K. Studies of the metallacrown complexes in solution show that they are stable and soluble in DMF and water. A proton relaxation study on complex **1** has revealed a relaxivity of 9.8 mM^{-1} s^{-1} (20 °C and 30 MHz), a value that is comparable to those of clinically useful MRI contrast enhancement agents. Complex **1** crystallizes in the triclinic space group $P\bar{1}$, with $a = 12.657(3)$ Å, $b = 14.833(3)$ Å, $c = 17.707(3)$ Å, $\alpha = 79.65(2)°$, $\beta = 86.06(2)°$, $\gamma = 68.69(2)°$, $V = 3046.6(12)$ Å, and $Z = 2$ (R1 = 0.0534, wR2 = 0.1289). Complex **2** crystallizes in the monoclinic space group $P2_1/n$, with $a = 16.319(2)$ Å, $b = 21.863(2)$ Å, $c = 18.410(3)$ Å, $\beta = 96.85(1)°$, $V = 6522(2)$ Å^3, and $Z = 4$ (R1 = 0.0463, wR2 = 0.0750). Complex **3** crystallizes in the triclinic space group $P\bar{1}$, with $a = 11.\ 173(6)$ Å, $b = 11.534(6)$ Å, $c = 13.311(5)$ Å, $\alpha = 93.81(3)°$, $\beta = 94.82(4)°$, $\gamma = 107.20(4)°$, $V = 1625(2)$ Å^3, and $Z = 2$ (R1 = 0.1230, wR2 = 0.2979).

In 1989 we reported the first of a new class of inorganic recognition agents which are now known as metallacrowns.[1−3] These molecules are composed of a central, high-density core which may contain a variety of metals in various oxidation levels.[4] The peripheries of the metallacrowns are formed with organic compounds that may vary in shape, functionality, and size.[5,6] The earliest metallacrowns utilized salicylhydroxamic acid (H_3shi) as the templating ligand and led to a rich variety of compounds in 9-metallacrown-3 (9-MC-3),[2,7] 12-metallacrown-4 (12-MC-4),[3,8−12] and 15-metallacrown-5 (15-MC-5)[13] motifs. We recognized that while H_3shi and related ligands led to high-yield, one-step syntheses of transition metal aggregates, the basic architecture of the ligand was not sufficiently versatile

[†] The University of Michigan.
[‡] The University of New Mexico.

(1) Pecoraro, V. *Inorg. Chim. Acta* **1989**, *155*, 171.
(2) Lah, M. S.; Kirk, M. L.; Hatfield, W.; Pecoraro, V. L. *J. Chem. Soc., Chem. Commun.* **1989**, 1606.
(3) Lah, M. S.; Pecoraro, V. L. *J. Am. Chem. Soc.* **1989**, *111*, 7258.
(4) Lah, M. S.; Pecoraro, V. L. *Comments Inorg. Chem.* **1990**,*11*, 59.
(5) Lah, M. S.; Pecoraro, V. L. *Inorg. Chem.* **1991**, *30*, 878.
(6) Pecoraro, V. L.; Stemmler, A. J.; Gibney, B. R.; Bodwin, J. J.; Wang, H.; Kampf, J. W.; Barwinski, A. Metallacrowns: A New Class of Molecular Recognition Agent. In *Progress in Inorganic Chemistry*; Karlin, K., Ed.; John Wiley & Sons: New York, 1997; Vol. 45, p 83.
(7) Gibney, B. R.; Stemmler, A. J.; Pilotek, S.; Kampf, J. W.; Pecoraro, V. L. *Inorg. Chem.* **1993**, *32*, 6008.
(8) Lah, M. S.; Gibney, B. R.; Tierney, D. L.; Penner-Hahn, J. E.; Pecoraro, V. L. *J. Am. Chem. Soc.* **1993**, *115*, 5857.
(9) Kurzak, B.; Farkas, E.; Glowiak, T.; Kozlowski, H. *J. Chem. Soc., Dalton Trans.* **1991**, 163.
(10) Gibney, B. R.; Kampf, J. W.; Kessissoglou, D. P.; Pecoraro, V. L. *Inorg. Chem.* **1994**, *33*, 4840.
(11) Stemmler, A. J.; Kampf, J. W.; Pecoraro, V. L. *Inorg. Chem.* **1995**, *34*, 2271.
(12) Gibney, B. R.; Wang, H.; Kampf, J. W.; Pecoraro, V. L. *Inorg. Chem.* **1996**, *35*, 184. Halfen, J.; Bodwin, J.; Pecoraro, V. L. *Inorg. Chem.* **1998**, *37*, 5416.
(13) Kessissoglou, D. P.; Kampf, J.; Pecoraro, V. L. *Polyhedron* **1994**, *13*, 1379.

10.1021/ic9800233 CCC: $18.00
Published on Web 05/19/1999

to access all desired metallacrown structure types. For example, while nonplanar 15-MC-5 could be prepared with H_3shi, a planar analogue of 15-MC-5 could not be accessed with this ligand because of the spatial restrictions imposed by having connected five- and six-membered chelate rings. We reasoned correctly that if a ligand was constructed with two adjacent five-membered chelates to bind the ring metals, planar 15-MC-5 that contained high-coordination-number central metals would result. This synthetic approach led to the first incorporation of an actinide into the central core of a metallacrown and also was the breakthrough necessary to allow for incorporation of chirality into the organic periphery of the complex.[14,15] Because of the generality of the synthetic approach, we can explore the physical properties of metallacrowns that contain transition metals in the ring which are linked by short bridges to lanthanides or actinides.

Polynuclear transition metal/lanthanide complexes have recently garnered significant attention due to the potential applications of these compounds as magnetic materials. Hopes for highly magnetic compounds stem from the interesting magnetic properties that result from the magnetic interactions between lanthanide ions and 3d transition metal ions.[16−22] For instance, it has been determined that Cu(II)−Gd(III) coordination complexes have an intramolecular interaction that is intrinsically ferromagnetic.[23] While several magnetic studies have focused on the interaction between copper(II) ion with lanthanides in the form of dimeric, trimeric, and tetrameric compounds,[23,29,30] there are no examples of a structural motif where five copper(II) ions surround a lanthanide ion in a planar arrangement. Precisely such a geometry is uniquely described by a planar 15-metallacrown-5. This type of structure potentially leads to a spin frustration in the copper ring which may impact the exchange interaction between the lanthanide and copper ions.

A growing application of gadolinium(III) coordination complexes is as magnetic resonance imaging (MRI) contrast agents.[23−28] Currently, $[Gd(DTPA)]^{2-}$ and $Gd(DOTA)^{-}$, with relaxivities of 3−7 mM^{-1} s^{-1}, are used as MRI contrast agents.[25] These molecules have the characteristic of enhancing the relaxation rate of water protons that are in close proximity to the Gd(III) ion. The differential proton relaxation rates between bulk water and the solvent associated with the contrast agent allow for the imaging of tissues in the MRI protocol.[26] Many factors affect the relaxivity of a molecule including the number of exchangeable coordinated waters, the rate of water exchange, and the tumbling time of the contrast agent. The next generation of contrast agents will likely exhibit much greater relaxivities than either $[Gd(DTPA)]^{2-}$ or $[Gd(DOTA)]^{-}$. Metallacrowns provide a basis for both increasing the number of exchangeable waters directly on the Gd(III) ion and generating adjacent sites on the ring metals that may keep water in close proximity to the central Gd(III).

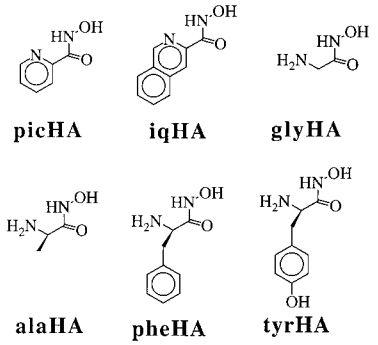

Figure 1. Structures of the ligands used in this study: H_2picha, H_2iqha, H_2glyha, H_2alaha, H_2pheha, and H_2tyrha.

In this contribution the generalized strategy for the preparation of planar 15-metallacrown-5 complexes is presented. The compounds are self-assembled in a facile one-step synthesis which is conveniently carried out in an open beaker in a fume hood. The 15-metallacrown-5 structure type forms a pentagonal-planar arrangement of 5 M(II) ions with a single lanthanide(III) or actinide(III) in the center. As will be shown, the resultant materials have interesting solid state magnetic properties, show significant water proton relaxivities, and can be prepared with as many as five resolved chiral centers. Some of these materials have been presented in previously published communications.[14,15]

Experimental Section

Materials. Ethyl picolinate, glycine hydroxamic acid, tyrosine hydroxamic acid, phenylalanine hydroxamic acid, leucine hydroxamic acid, copper(II) acetate, gadolinium(III) nitrate, erbium(III) nitrate, ytterbium(III) nitrate, lanthanum(III) nitrate, europium(III) nitrate, samarium(III) nitrate, dysprosium(III) nitrate, holmium(III) nitrate, neodymium(III) nitrate, hydroxylamine hydrochloride, and potassium hydroxide were obtained from Aldrich Chemical Co. HEPES buffer was used as obtained from US Biochemical Corporation. Ultrapure Tris buffer was used as obtained from Bethesda Research Laboratories. Disodium ethylenediaminetetraacetic acid (Na_2H_2EDTA) was purchased from Fischer Scientific. All other chemicals and solvents were reagent grade.

Abbreviations used: H_2picha = picoline hydroxamic acid; H_2iqha = isoquinoline hydroxamic acid; H_2glyha = glycine hydroxamic acid; H_2L-alaha = L-alanine hydroxamic acid; H_2L-tyrha = L-tyrosine hydroxamic acid; H_2pheha = phenylalanine hydroxamic acid; H_2leuha = leucine hydroxamic acid; Me_4[l4]aneN_4 = *N*,*N*′,*N*″,*N*‴-1,4,8,11-tetraazacylcodecane; H_5DTPA = diethylenetriaminepentaacetic acid pentaanion; H_4DOTA = 1,4,7,10-tetraazacyclododecane *N*,*N*′,*N*″,*N*‴-1,4,7,10-tetraacetic acid tetraanion; H_3nha = naphthoylhydroxamic acid; H_2anha = anthranilic hydroxamic acid.

Preparation of Ligands. The ligands used in this study are shown as Figure 1. Picoline hydroxamic acid, H_2picha, was prepared as

(14) Stemmler, A. J.; Kampf, J. W.; Pecoraro, V. L. *Angew. Chem., Int. Ed. Engl.* **1996**, *35*, 2841.
(15) Stemmler, A. J.; Barwinski, A.; Kampf, J. W.; Young, V.; Pecoraro, V. L. *J. Am. Chem. Soc.* **1996**, *118*, 11962.
(16) Bencini, A.; Benelli, C.; Caneschi, A.; Carlin, R. L.; Gatteschi, D. *J. Am. Chem. Soc.* **1985**, *107*, 8128.
(17) Bencini, A.; Benelli, C.; Caneschi, A.; Del, A.; Gatteschi, D. *Inorg. Chem.* **1986**, *25*, 572.
(18) Benelli, C.; Bencini, A.; Caneschi, A.; Gatteschi, D.; Pardi, L.; Rey, P.; Shum, D. P.; Carlin, R. L. *Inorg. Chem.* **1989**, *28*, 272.
(19) Benelli, C.; Caneschi, A.; Gatteschi, D.; Guillou, O.; Pardi, L. *Inorg. Chem.* **1990**, *29*, 1750.
(20) Blake, A. J.; Gould, R. O.; Milne, P. E. Y.; Winpenny, R. E. P. *J. Chem. Soc., Chem. Commun*. **1991**, 1453.
(21) Sanz, J. L.; Ruiz, R.; Gleizes, A. L., F.; Faus, J.; Julve, M.; Borras-Almenar, J. J.; Journaux, Y. *Inorg. Chem.* **1996**, *35*, 7384.
(22) Ramade, I.; Kahn, O.; Jeannin, Y.; Robert, F. *Inorg. Chem.* **1997**, *36*, 930.
(23) Aime, S.; Botta, M.; Geninatti, C.; Giovenzana, G. B.; Jommi, G.; Pagliarin, R.; Sisti, M. *J. Chem. Soc., Chem. Commun*. **1995**, 1885.
(24) Aime, S.; Botta, M.; Ermondi, G.; Terreno, E.; Anelli, P. L.; Fedeli, F.; Uggerl, F. *Inorg. Chem.* **1996**, *35*, 2726.
(25) Lauffer, R. B. *Chem. Rev.* **1987**, *87*, 901.
(26) Runge, V. M. In *Enhanced Magnetic Resonance Imaging*; Runge, V. M., Ed.; C. V. Mosby Co.: St. Louis, MO, 1989.
(27) Kim, W. D.; Kiefer, G. E.; Maton, F.; McMillan, K.; Muller, R. N.; Sherry, A. D. *Inorg. Chem.* **1995**, *34*, 2233.
(28) Moonen, C. T. W.; Van Zijl, P. C. M.; Frank, J. A.; Bihan, D. L.; Becker, E. D. *Science* **1990**, *250*, 53.
(29) (a) Costes, J.; Dahan, F.; Dupois, A.; Laurent, J. *Inorg. Chem.* **1996**, *35*, 2400. (b) Costes, J.; Dahan, F.; Dupois, A.; Laurent, J. *Inorg. Chem.* **1997**, *36*, 3429.
(30) Chen, L.; Breeze, S. R.; Rousseau, R. J.; Wang, S.; Thompson, L. K. *Inorg. Chem.* **1995**, *34*, 454.

previously described.[32] A general method was used for the preparation of hydroxamates[33] which is described specifically for isoquinoline hydroxamic acid, H_2iqha. After cooling to room temperature, solutions containing 32.1 mmol of $NH_2OH{\cdot}HCl$ dissolved in 10.1 mL of MeOH and 32.1 mmol of KOH dissolved in 15 mL of MeOH were mixed under a layer of N_2 in an ice bath. Precipitation of KCl was allowed to occur for 5 min, and then the salt was removed by filtration. Isoquinoline ethyl ester (10.7 mmol) was added to the free hydroxylamine, and the solution was covered and then stirred for 18 h. A yellow, gelatinous material which initially precipitated was redissolved in approximately 30 mL of 1.25 N acetic acid in MeOH. After 6 h at 4 °C, large white crystals of the isoquinoline hydroxamic acid were isolated, washed with ethanol, and dried in a vacuum (62% yield). The crystals were characterized by elemental analysis and ^{1}H and ^{13}C NMR. Anal. Calcd for $C_{10}H_8N_2O_2$ (MW = 188): C, 63.83; H, 4.25; N, 14.89. Found: C, 63.68; H, 4.50; N, 14.84. ^{1}H NMR (CD_3OD): δ (ppm) 9.23, 8.46, 8.13, 8.05, 7.83, 7.76. ^{13}C(CD_3OD): 164.837, 153.18, 144.43, 137.29, 132.65, 131.38, 130.49, 129.11, 129.03, 121.23.

Preparation of Complexes. In addition to the specific compounds described below, several other metallacrowns (compiled in Table S1, Supporting Information) have been prepared with picoline hydroxamic acid and copper(II) using different lanthanide ions encapsulated in the center (with La(III), Nd(III), Sm(III), Ho(III), Dy(III), Er(III), and Yb(III)). The following complexes have varying numbers of associated solvent molecules that affect their elemental analyses.

{$Gd(NO_3)_3[Cu^{II}(picha)]_5(DMF)_5$}, $Gd(NO_3)_3$[15-$MC_{Cu(II)N(picha)}$-5], 1, and {$Eu(NO_3)_3[Cu^{II}(picha)]_5(DMF)_6$}, $Eu(NO_3)_3$[15-$MC_{Cu(II)N(picha)}$-5], 2. A 50 mL DMF solution of $Cu(OAc)_2$ (0.40 g, 2 mmol) was mixed with a 50 mL DMF solution of H_2picha (0.28 g, 2 mmol), and the resultant solution was stirred for 1 h. $Gd(NO_3)_3$ (0.13 g, 0.4 mmol) was added to the solution, causing a slight change in color to a darker green. Vapor diffusion with ether resulted in a 76% yield of dark green rhombic crystals of **1**. Elemental anal. Calcd for $Cu_5C_{32}H_{23}N_{13}O_{21}Gd$ (MW = 1400): Cu, 22.5; C, 27.15; H, 1.98; N, 12.86. Found: Cu, 22.3; C, 27.38; H, 2.30; N, 12.49. FAB+MS gave a molecular ion of 1275 *m*/*e* (7.5% of base), 1214 (5.8%), 607 (5.6%) intact ion in DMF. The same procedure using $Eu(NO_3)_3$ (0.18 g, 0.4 mmol) followed by slow evaporation of the solvent, rather than vapor diffusion, resulted in a 79% yield of dark green rhombic crystals of **2**. Elemental anal. Calcd for $Cu_5C_{44}H_{54}N_{17}O_{23}Eu$: Cu, 19.2; C, 31.9; H, 3.3; N, 14.4. Found: Cu, 19.6; C, 31.81; H, 3.25; N, 14.51. FAB+MS gave $[M]^+$ of 1273 *m*/*z*, $[M]^{2+}$ of 1211 *m*/*z* and 606 *m*/*z* in DMF.

{$Eu(NO_3)_2(OH)[Cu^{II}(glyha)]_5(H_2O)_8$}, $Eu(NO_3)_3$[15-$MC_{Cu(II)N(glyha)}$-5], 3. A 50 mL aqueous solution of $Cu(OAc)_2$ (0.40 g, 2 mmol) and $Eu(NO_3)_3$ (0.18 g, 0.4 mmol) was mixed with a 50 mL aqueous solution of H_2glyha (0.18 g, 2 mmol). Since the ligand did not dissolve, tetraethylammonium hydroxide (25% in water) was added to achieve pH 7 (approximately 3−4 mL), at which point the solution changed from green to purple. Slow evaporation of solvent resulted in purple needle crystals (47% yield). Elemental anal. Calcd for $Cu_5C_{14}H_{42}N_{18}O_{20}$-Eu (MW = 1252): Cu, 27.2; C, 14.38; H, 3.68; N, 13.18. Found: Cu, 26.6; C, 14.12; H, 3.32; N, 12.36. FAB+MS gave $[M]^+$ of 1033 *m*/*z*, $[M]^{2+}$ of 971 *m*/*z* and 486 *m*/*z* in DMF in a 3-nitrobenzyl alcohol matrix.

{$UO_2(NO_3)_3[Cu^{II}(picha)]_5(DMF)$}, $UO_2(NO_3)_3$[15-$MC_{Cu(II)N(picha)}$-5], 4, and {$Nd(NO_3)_2(OH)[Cu^{II}$(L-alaha)$]_5(H_2O)_{16}$}, $Nd(NO_3)_2$(OH))[15-$MC_{Cu(II)\ N(L-alaha)}$-5], 5. These metallacrowns were synthesized and characterized as previously described.[14,15]

{$Gd(NO_3)_3[Cu^{II}(iqha)]_5(DMF)_4$}, $Gd(NO_3)_3$[15-$MC_{Cu(II)N(iqha)}$-5], 6, and {$Eu(NO_3)_3[Cu^{II}(iqha)]_5(DMF)$}, $Eu(NO_3)_3$[15-$MC_{Cu(II)N(iqha)}$-5], 7. The procedure for compound 1, substituting H_2iqha (0.28 g, 2 mmol) for H_2picha, gave, after stirring for 12 h, a greenish gray microcrystalline solid in 63.5% yield. Elemental anal. Calcd for $Cu_5C_{59}H_{51}N_{16}O_{22}Gd$ (MW = 1810): Cu, 17.5; C, 39.13; H, 2.84; N, 12.37. Found: Cu, 17.2; C, 39.18; H, 3.01; N, 12.12. Due to low solubility, mass spectral data are not available. The procedure for compound 2, substituting H_2-iqha (0.28 g, 2 mmol) for H_2picha, gave an army green to forest green solution. Vapor diffusion with ether resulted in an 85.8% yield of dark green rhombic crystals. Elemental anal. Calcd for $Cu_5C_{54}H_{41}N_{14}O_{21}Eu$ (MW = 1691): Cu, 18.8; C, 38.32; H, 2.42; N, 11.59. Found: Cu, 19.0; C, 38.84; H, 2.91; N, 11.78. Due to low solubility, mass spectral data are not available.

{$Ca(NO_3)_3[Cu^{II}(picha)]_5(DMF)$}, $Ca(NO_3)_3$[15-$MC_{Cu(II)N(picha)}$-5], 8. This metallacrown was synthesized and characterized as previously described.[14]

{$Gd(NO_3)_3[Ni^{II}(picha)]_5(DMF)$}, $Gd(NO_3)_3$[15-$MC_{Ni(II)N(picha)}$-5], 9. $Ni(OAc)_2$ (0.49 g, 2 mmol) was dissolved in 50 mL of DMF. H_2picha (0.28 g, 2 mmol) dissolved in 50 mL of DMF was added to the solution, which was stirred for 1 h. $Gd(NO_3)_3$ (0.18 g, 0.4 mmol) was added to the dark reddish-yellow solution. This solution was dried with a stream of N_2 gas. The residue was redissolved in methanol. A yellow green precipitate in a 34% yield was obtained after evaporation of solvent. Elemental anal. Calcd for $Ni_5C_{33}H_{62}N_{13}O_{37}Gd$ (MW = 1682): Ni, 17.43; C, 23.54; H, 3.71; N, 10.82. Found: Ni, 17.0; C, 23.56; H, 3.40; N, 10.56. FAB+MS in a 3-nitrobenzyl alcohol matrix gave a molecular ion of 1254 *m*/*e* in DMF.

{$Nd(NO_3)_3[Ni^{II}(picha)]_5(DMF)$}, $Nd(NO_3)_3$[15-$MC_{Ni(II)N(picha)}$-5], 10. A 50 mL DMF solution of $Ni(OAc)_2$ (0.49 g, 2 mmol) was mixed with a 50 mL DMF solution of H_2picha (0.28 g, 2 mmol), and the resultant solution was stirred for 1 h. $Nd(NO_3)_3$ (0.17 g, 0.4 mmol) was added to this dark reddish-yellow solution, which was then taken to dryness using a stream of N_2 gas. The residue was redissolved in methanol, and a yellow green precipitate was recovered in a 32% yield upon evaporation of solvent. Elemental anal. Calcd for $Ni_5C_{34}H_{64}N_{13}O_{37}$-Nd (MW = 1683): Ni,17.42; C, 24.24; H, 3.83; N, 10.81. Found: Ni, 17.0; C, 24.09; H, 3.39; N, 11.28. FAB+MS in a 3-nitrobenzyl alcohol matrix gave a molecular ion of 1240 *m*/*e* in DMF.

Methods

NMR Spectroscopy. ^{1}H NMR spectra were recorded on Bruker 200 or 360 MHz FT-NMR spectrometers operating in the quadrature detection mode. Samples were dissolved in 98% deuterated solvents. Chemical shifts were referenced to TMS or solvent peaks. A sweep width of 100 000 with 1000 transients was used to detect paramagnetically shifted proton peaks. The spectra were collected with 8K data points. To increase the signal-to-noise ratio, the free induction decay was transformed using a ~20 Hz exponential apodization. Deuterated NMR solvents (CD_3OD, D_2O, DMSO-d_6) were obtained from Cambridge Isotope Laboratories.

Proton relaxation rates were determined on a home-built NMR relaxation spectrometer at a proton Larmor frequency of 30 MHz. The sample temperature was maintained at 19 °C. Proton T_1 relaxation rates were measured using the phase-shifted triplet inversion−recovery method.[34] The triplet sequence samples the proton magnetization during the decay and restores it to the *z*-axis so that T_1 can be determined from the decay following a single inverting pulse. The relaxivity was determined by a serial dilution in water covering a range of 0.5−0.015 mM. The relaxation rate was plotted versus concentration with the slope of the fit line giving the relaxivity.

UV/Vis and Circular Dichroism Spectroscopies. UV/vis spectra were recorded on a Perkin-Elmer Lambda 9 UV/vis/near-IR spectrophotometer interfaced to a 486 PC. Circular dichroism (CD) spectra were recorded on an AVIV 62DS spectrometer using a 1 cm path length cuvette. For each sample, 501 data points were collected at a rate of 1 point/s. The temperature of the experiments was maintained at either 25 or 37 °C. Each spectrum was collected from 240 to 800 mm.

(31) Gatteschi, D.; Caneschi, A.; Pardi, L.; Sessoli, R. *Science* **1994**, *265*, 1054.
(32) Hase, J.; Kobashi, J.; Kawaguchi, K.; Sakamoto, K. *Chem. Pharm. Bull.* **1971**, *19*, 363.
(33) Blatt, A. H. In *Organic Syntheses*; Blatt, A. H., Ed.; Wiley: New York, 1943; Collect. Vol. II, p 67.
(34) Bovet, J. M. In *Proton NMR Relaxation Enhancements due to Manganese in the Photosynthetic Oxygen Evolving Complex*; Bovet, J. M., Ed.; University of Michigan: Ann Arbor, MI, 1993.

Experiments were completed both in the absence and in the presence of buffer (either Tris or HEPES) with the pH maintained at 7.0. Identical results were obtained in the presence or absence of buffers. The concentration of metallacrowns was 5.7 mM in pure aqueous solution and 1.0 mM in HEPES-buffered (10 mM) solutions. To test the acid stability of the metallacrowns, these solutions were subjected to the addition of excess 1 M nitric acid lowering the pH to approximately 2. Addition of excess Cu(II) or ligand was accomplished by titration of stock solutions into 10 mM solutions of metallacrown.

Magnetism. Estimates of the magnetic moment of five isolated Cu(II) ions were calculated using the following equation:

$$\mu_{\text{eff}} = g\sqrt{\sum S_i(S_i + 1)}$$

The symbols are given as $S_i = S_1 = S_2 = S_3 = S_4 = S_5 = {}^1/_2$ and $g = 2.1$ (a value that is consistent with other Cu(II) complexes). The variable-temperature magnetic susceptibility data was used to determine the magnetic moment of the 15-metallacrown-5 structures according to

$$\mu_{\text{eff}} = 2.828\sqrt{\chi T}$$

Variable-temperature magnetic susceptibility data were obtained on a Quantum Concepts SQUID magnetometer. Susceptibility data were collected from 4 to 300 K at 0.5*T* and corrected for diamagnetism using Pascal's constants.[35] Saturation magnetization studies were performed at 2, 4, and 8 K at fields from 100 to 50 000 G. The saturation magnetization data, presented as plots of *H*[applied]/*T* versus magnetization, were fit with the Brillouin function for a particular spin state ($S' = {}^1/_2$ and $S' = {}^7/_2$). The Brillouin function is shown below where $x = -C\beta H/kT$.

$$\chi M = -\frac{N}{H} g S' \beta \left[\frac{2S'+1}{2S'} \coth\left(\frac{S'(2S'+1)}{2S'} \right) x - \frac{1}{2S'} \coth\left(\frac{x}{2} \right) \right]$$

The variable-temperature magnetic susceptibility data were fit using the Curie Law, where $\chi = C/T$ and $C = (Ng^2\beta^2/3k)(S(S + 1))$. Curve-fitting analysis was done using a nonlinear least-squares fitting analysis available in the KaleidaGraph program.

Mass Spectroscopy. Positive and negative fast atom bombardment ionization (FAB) mass spectra were acquired by the University of Michigan Mass Spectroscopy Facility for the metallacrowns in DMF or methanol using a 3-nitrobenzyl alcohol matrix. Positive and negative electrospray ionization (ESI) mass spectra were acquired by the University of Michigan Protein and Carbohydrate Structure Facility for metallacrowns dissolved in water or methanol. Elemental analyses were performed by the Microanalysis Laboratory in the Department of Chemistry at the University of Michigan.

Collection and Reduction of X-ray Data. Suitable crystals of **1**−**3** were obtained as described above and mounted in glass capillaries. Intensity data were collected on a Siemens P4U diffractometer (equipped with LT-2) or a Siemens R3m/V diffractometer using Mo Kα radiation (0.7107) monochromatized from a graphite crystal. Three standard reflections measured every 97 reflections set were used for scaling the data. Crystal and data parameters are given in Table 1. The data were reduced using either the SHELXTL PLUS program package or the SHELX-93 program package on a VAX Station 3500.[36,37] The structures were solved via the Patterson method and the model refined with full-matrix least squares on F^2. The agreement indices, $R1 = \sum||F_o| - |F_c||/\sum|F_o|$ and $wR2 = [\sum w(F_o^2 - F_c^2)/\sum w(F_o)^2]^{1/2}$, were used to evaluate the results. Atomic scattering factors were taken from the *International Table for X-ray Crystallography*.[38] Unique data and final *R* indices are given in Table 1. The fractional atomic coordinates and anisotropic thermal parameters of all non-hydrogen atoms for **1**−**3** can be found in the Supporting Information. Selected average interatomic bond distances and angles for **1**−**3** are given in Tables 2 and 3, respectively. The structural parameters of **1**−**3** will be compared to the previously synthesized and characterized complexes, **4** and **5**. Complete crystallographic details are given in the Supporting Information.

Table 1. Summary of Crystallographic Data for **1**−**3**

	1	**2**	**3**
empirical formula	$C_{45}H_{55}N_{18}O_{24}Cu_5Gd\cdot 0.25H_2O$	$C_{45}H_{55}N_{19}O_{25}Cu_5Eu$	$C_{10}H_{37}Cu_5N_{12}O_{25}Eu$
fw (amu)	1711	1715	1196
space group	$P\bar{1}$ (No. 2)	$P2_1/n$ (No. 14)	$P\bar{1}$ (No. 2)
a, Å	12.657(3)	16.319(2)	11.173(6)
b, Å	14.833(3)	21.863(2)	11.534(6)
c, Å	17.707(3)	18.410(3)	13.311(5)
α, deg	79.65(2)	90	93.81(3)
β, deg	86.06(2)	96.85(1)	94.82(4)
γ, deg	68.69(2)	90	107.20(4)
V, Å^3	3046.6(12)	6522(2)	1625
Z	2	4	2
D_{calc}, mg/m^3)	1.865	1.747	2.425
temp, °C	178	178	178
μ, cm^{-1}	28.81	26.38	52.29
R1 (wR2)[a]	0.0534 (0.1289)	0.0463 (0.0750)	0.1230 (0.2979)

[a] Structure was refined on F^2 using $R1 = \sum||F_o| - |F_c||/\sum|F_o|$ and $wR2 = [\sum w(F_o^2 - F_c^2)/\sum w(F_o)^2]^{1/2}$.

Results

Description of $Gd(NO_3)_2[15\text{-}MC_{Cu(II)N(picha)}\text{-}5]\}NO_3(DMF)_5$, 1. The model for $Gd(NO_3)_2[15\text{-}MC_{Cu(II)N(picha)}\text{-}5]^+$, obtained by analysis of triclinic crystals, is shown in Figure 2. The hydroximate nitrogen and oxygen atoms from each of the five picha^{2-} ligands and the five Cu(II) ions form a ring based on the M−N−O−M linkage; this ring is outlined in bold in Figure 2. The metallacrown ring is formally neutral since the positive (+2) charges of the copper(II) ions are balanced by the negative charge (−2) of the picha^{2-}. A Gd(III) ion is encapsulated at the center of the structure with the positive charge being balanced by three nitrate ions. One nitrate anion is bound in a bidentate fashion to the Gd(III) ion, and a second nitrate anion is bound to a copper(II) ion (Cu4). The third nitrate is present in the crystal lattice along with an unbound DMF molecule (not shown).

Four of the five ring Cu(II) ions are five-coordinate, and the fifth Cu(II) is four-coordinate. On one face of the metallacrown ring, two DMF oxygen atoms, O15 and O20, are bound to Cu2 and Cu5, respectively; and one DMF oxygen, O14, is bound to Gd(III). On the opposite face of the metallacrown, one DMF oxygen, O16, is bound to Cu3. The bound solvent and anion molecules complete a five-coordinate, square-pyramidal coordination of the individual copper ions in the ring. The Cu1, which contains ligands solely from two picha^{2-} molecules,

(35) Drago, R. *Physical Methods in Chemistry*; Harcourt Brace Jovanovich: 1992.
(36) Sheldrick, G. M. 1988, 3.43/V.
(37) Sheldrick, G. M. *SHELXL-93 Program for crystal structure refinement*; University of Gottingen: Gottingen, Germany, 1993.
(38) Wilson, A. J. *International Tables for crystallography*; Kluwer Academic Publishers: Dordrecht, The Netherlands, 1992; Vol. C.

Table 2. Comparison of Structural Parameters for Copper 15-Metallacrown-5 Structures[a]

distances	**1**	**2**	**3**	**4**	**5**	Cu^{II}[12-MC-4]
Cu−Ln(core)	3.894(5)	3.904(5)	3.898(10)	3.894(5)	3.966(5)	3.273(2)
Cu−M(ring)	4.584(5)	4.580(6)	4.582(11)	4.624(5)	4.614(5)	4.611(1)
Ln−O(oxime)	2.411(5)	2.427(6)	2.445(11)	2.402(5)	2.532(4)	1.901(3)
Cu−O(oxime)	1.928(5)	1.933(6)	1.921(11)	1.953(5)	1.934(5)	1.910(3)
Cu−O(carbonyl)	1.944(5)	1.933(6)	1.956(11)	1.952(5)	1.952(5)	1.947(2)
Cu−N(imine)	1.914(6)	1.938(7)	1.907(13)	1.924(6)	1.918(5)	1.914(4)
Cu−N(pyr or amine)	2.004(6)	1.991(7)	1.999(13)	2.002(6)	2.022(6)	1.895(3)
Cu−O(sol)	2.306(6)	2.299(6)	2.442(14)	2.316(5)	2.570(6)	2.323(3)
Ln−O(NO_3 or oxo)	2.455(5)	2.517(6)	2.380(13)	1.755(5)		
Ln−O(sol)	2.390(5)		2.390(12)		2.537(5)	
Ln−O(plane)	0.56	0.04	0.30	0.01	0.64	0.05
cavity radius	1.12	1.13	1.14	1.13	1.17	0.56

[a] Cu^{II}[12-MC-4] = an average of the similar bond lengths for four copper metallacrowns: $[Cu^{II}12\text{-}MC_{Cu(II)N(anha)}\text{-}4](ClO_4)_2$; $(TEA)_2[Cu^{II}12\text{-}MC_{Cu(II)N(nha)}\text{-}4]$; $(Na\cdot15\text{-}C\text{-}5)_2\{Cu^{II}[12\text{-}MC_{Cu(II)N(shi)}\text{-}4]\}$ and $(TMA)_2\{Cu^{II}[12\text{-}MC_{Cu(II)N(shi)}\text{-}4]\}$.[29]

Table 3. Comparison of the Range of Selected Angles (deg) for Copper 15-Metallacrown-5 Structures[a]

metallacrown	**1**	**2**	**3**	**4**	**5**	Cu^{II}[12-MC-4]
O(oxime)−M(ring)−O(carbonyl)	85.7(2)−86.0(2)	84.9(2)−86.6(2)	84.3(2)−85.8(2)	83.7(2)−85.2(2)	84.7(2)−85.1(2)	80.4(6)−81.5(5)
O(oxime)−M(ring)−N(imine)	89.0(2)−90.2(2)	89.3(2)−92.6(2)	89.9(2)−91.1(2)	87.0(2)−91.1(2)	90.5(2)−92.2(2)	89.3(5)−93.1(5)
N(imine)−M(ring)−N(pyr or amine)	80.3(2)−81.1(2)	80.5(2)−82.2(5)	81.8(2)−84.1(2)	80.1(2)−79.6(2)	82.1(2)−83.3(2)	91.8(5)−94.7(5)
N(pyr or amine)−M(ring)−O(carbonyl)	101.8(2)−103.8(2)	98.7(2)−102.6(2)	99.1(2)−101.7(2)	100.5(2)−105.6(2)	99.5(2)−101.4(2)	91.9(6)−96.5(5)
M(ring)− O(oxime)−M(core)	126.4(2)−128.7(2)	122.8(2)−129.2(2)	123.4(2)−125.7(2)	124.7(2)−128.7(2)	123.1(2)−125.9(2)	116.2(6)−121.4(7)
O(oxime)−M(core)−O(oxime)	70.6(2)−72.5(2)	70.7(2)−74.0(2)	70.6(2)−72.7(2)	69.9(2)−73.7(2)	67.57(14)−70.42(14)	86.5(5)−92.6(5)

[a] Cu^{II}[12-MC-4] = $(Na\cdot15\text{-}C\text{-}5)_2\{Cu^{II}[12\text{-}MC_{Cu(II)N(shi)}\text{-}4]\}$.[29]

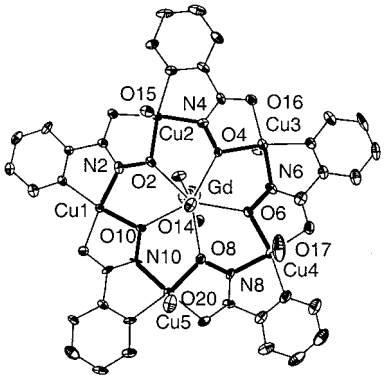

Figure 2. ORTEP diagram of **1**. The [15-MC-5] ring is outlined in bold. Thermal ellipsoids are at 50% probability.

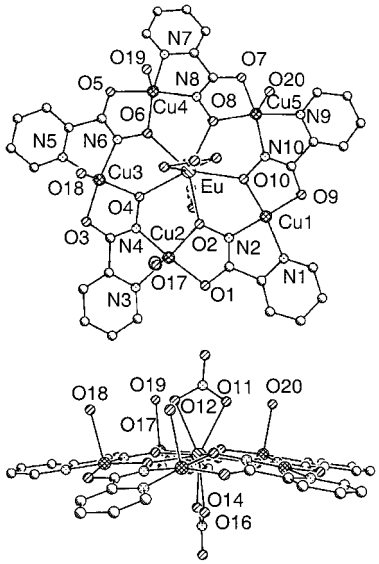

Figure 3. Pluto diagram of **2**, $Eu(NO_3)_3[15\text{-}MC_{Cu(II)N(picha)}\text{-}5]$, top and side views.

remains four-coordinate, square-planar. Each copper ion is bound in five-membered chelate rings composed of either a carbonyl oxygen and an oxime oxygen or an imine nitrogen and pyridine nitrogen. The average Cu−N(pyr) distance, 2.004 Å, is longer than the Cu−O(carbonyl), Cu−O(oxime), and Cu−N(imine) distances of 1.928, 1.944, and 1.914 Å, respectively. The solvent anions are only weakly bound to the copper ions with an average distance of 2.31 Å.

The gadolinium ion is eight-coordinate including the five metallacrown ring oxygen donors, bound solvent, and nitrate. The lanthanide ion to oxime oxygen distances, average 2.411 Å, are slightly shorter than the Gd(III)−O (O from NO_3^- or solvent) distance of 2.455 Å. The Gd(III) coordination sphere closely approximates a pentagonal bipyramid.[39] The gadolinium ion is displaced 0.256 Å out of the best least-squares plane of the five oxygen donor atoms of the metallacrown ring toward the bidentate nitrate. The calculated cavity radius of this metallacrown (1.12 Å) and the ionic radius of eight-coordinate Gd(III) (1.05 Å) are in good agreement.

Description of $\{Eu(NO_3)_2[15\text{-}MC_{Cu(II)N(picha)}\text{-}5](DMF)_4\}\cdot NO_3\cdot 2DMF$, 2. The PLUTO diagram of $Eu(NO_3)_2[15\text{-}MC_{Cu(II)N(picha)}\text{-}5]$, shown as Figure 3, illustrates that this 15-metallacrown-5 ring deviates slightly from planarity, giving the cation a distinct bowl shape. The curvature arises from the fact that four of the copper ions are square-pyramidal with their axial ligands all on one face of the metallacrown. These axial ligands are DMF oxygen donors, O17, O18, O19, and O20 bound to Cu2, Cu3, Cu4, and Cu5. The solvent is only weakly bound with an average bond length of 2.299 Å for the four Cu−O_{sol}

(39) Bligh, S. W. A. *J. Chem. Soc., Dalton Trans.* **1994**, 3369.

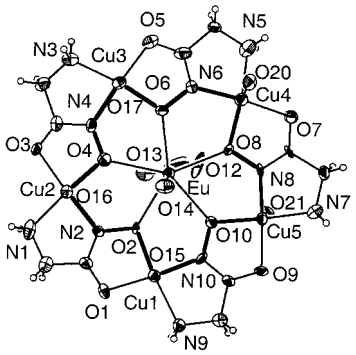

Figure 4. ORTEP diagram of **3** with thermal ellipsoids at 50%. The [15-MC-5] ring is outlined in bold.

distances. Similar to **1**, one of the four copper(II) ions, Cu1, is four-coordinate in a square-planar configuration.

Two bidentate nitrate anions are bound to europium(III) on either side of the metallacrown ring. The Eu(III) is essentially pentagonal-bipyramidal with rather long bonds to the nitrates above and below the ring, 2.517 Å, and shorter bonds to the five metallacrown oxygen donors, an average of 2.427 Å. The bite angle of the metallacrown oxygen donors, O(oxime)−M(core)−O(oxime), is ∼ 72°, consistent with a planar pentagon. There are two DMF molecules and one nitrate anion that are present in the crystal lattice. The close agreement between cavity radius, 1.17 Å, and the ionic radius of Eu(III), nine-coordinate, 1.13 Å, results in an encapsulated ion that is bound directly in the least-squares plane of the five oxygen donors of the metallacrown.

Description of $\{Eu(NO_3)_2OH[15\text{-}MC_{Cu(II)N(glyha)}\text{-}5](H_2O)_4\}\cdot 4H_2O$, 3. This metallacrown was synthesized in water and, as shown in Figure 4, contains inner-sphere coordination of water to the lanthanide ion. All five copper(II) ions have a weak axial bond to water with an average bond length of 2.442 Å, lengths that are much longer than the axial bonds in **1**, **2**, **4** and **5**. Despite having all copper(II) ions in a square-pyramidal environment, the metallacrown ring has less buckling than **1** probably due to weaker binding to the axial ligands.

The structure of **3** was solved to an $R = 12.3\%$. The high residual was due to disorder in the eight water molecules in the structure. There are four water molecules and one hydroxide bound to either a Cu(II) or Eu(III) ion. The hydroxide anion is necessary to achieve charge balance, although the position of the hydroxide cannot be assigned because the hydrogen atoms were not placed for the hydroxide or water molecules in solving the crystal structure. One monodentate nitrate, O17, is bound to Cu3 while water oxygen donors, O20 and O15 are bound to Cu4 and Cu1 (not visible on the ORTEP diagram). These axial ligands are all on one face of the metallacrown ring. Two water oxygen donors, O16 and O21, are bound to Cu2 and Cu5 on the same side of the ring as the bidentate nitrate that is bound to Eu(III). As expected the coordination of the amine in place of the pyridine nitrogen leads to the same bond distance: Cu−N(pyr) for **1** and **2** averages 2.004 and 1.991 Å, respectively, and Cu−N(amine) for **3** is 1.999 Å.

In this structure the Eu(III) ion is only eight-coordinate with the literature value of an ionic radius of 1.07 Å. The Eu(III) ion is displaced from the least-squares plane by 0.3 Å toward the bidentate nitrate. The metallacrown has a cavity radius of 1.14 Å and a bite angle of (approximately) 72°.

This molecule has an interesting network of hydrogen bonds surrounding the metallacrown. The nitrate that is bound to Eu(III) has hydrogen bonds to two waters that are bound to copper(II) ions, Cu2 and Cu5. A similar effect is found on the other face of the metallacrown. The hydroxide that is bound to Eu(III) is hydrogen bonded to a water that is bound to Cu1. Also a hydrogen bond is formed with a water in the lattice that is then hydrogen bonded to a water that is bound to Cu4.

Solution Characterization. Spectroscopic Studies. The solution speciation of the planar 15-metallacrown-5 structures was investigated by solution mass spectrometry. A FAB-MS^- of **1** in DMF in a 3-nitrobenzyl alcohol matrix gave molecular ion peaks and an intact ion peak at 1275 *m*/*e*, 1214 *m*/*e*, and 607 *m*/*e* corresponding to $\{Gd(NO_3)_2[15\text{-}MC_{Cu(II)N(picha)}\text{-}5]\}^+$ and $\{Gd(NO_3)[15\text{-}MC_{Cu(II)N(picha)}\text{-}5]\}2^+$, respectively. FAB-$MS^+$ of $Eu(NO_3)_3[15\text{-}MC_{Cu(II)N(picha)}\text{-}5]$ gave $[M]^+$ of 1273 *m*/*e*, $[M]^{2+}$ of 1211 *m*/*e* and 606 *m*/*e* in DMF in a 3-nitrobenzyl alcohol matrix. The FAB-MS^+ spectrum of **2** is presented as Figure S1 (Supporting Information). FAB-MS^+ spectra containing peaks with mass-to-charge ratios corresponding to one or two nitrate ions associated with each metallacrown are observed for all of the $[15\text{-}MC_{Cu(II)N(picha)}\text{-}5]$ metallacrowns in DMF (where the lanthanide ions, La(III), Nd(III), Sm(III), Eu(III), Gd(III), Dy(III), Ho(III), and Er(III), are bound) as shown in Table S1. $Yb(NO_3)_3[15\text{-}MC_{Cu(II)N(picha)}\text{-}5]$ was insoluble in DMF (the solubility of the metallacrowns in DMF seems to decrease in the series from La(III) to Yb(III)), but a similar spectrum was obtained for this compound in methanol by FAB-MS^+. Similar patterns of peaks corresponding to mass-to-charge ratios that contain one or two nitrate ions associated with the metallacrown are observed for $[15\text{-}MC_{Ni(II)N(picha)}\text{-}5]$ structures with Gd(III) and Nd(III), **9** and **10**, in a DMF solution by FAB-MS^+.

Electrospray ionization mass spectroscopy has been shown to be effective in identifying the speciation of ions in solution and was applied to several of the $[15\text{-}MC_{Cu(II)N(picha)}\text{-}5]$ structures.[27,28] This soft ionization technique has proven useful in providing the solution molecular weights of the formally neutral metallacrown salt complexes after the loss of bound anions.[29,30] A methanol solution of $Gd(NO_3)_3[15\text{-}MC_{Cu(II)N(picha)}\text{-}5]$ gave an intact ion peak at 607 *m*/*e* and the molecular ion peak at 1274 *m*/*e* corresponding to $\{Gd(NO_3)[15\text{-}MC_{Cu(II)N(picha)}\text{-}5]\}^{2+}$ and $\{Gd(NO_3)_2[15\text{-}MC_{Cu(II)N(picha)}\text{-}5]\}^+$, respectively, shown as Figure S2 (Supporting Information). It was not possible to obtain satisfactory ESI-MS^+ spectra of either **1** or **2** in water, possibly because these spectra were taken at a high repeller voltage or due to low solubility. The ESI-MS^+ spectrum of $Nd(NO_3)_3[15\text{-}MC_{Cu(II)N(picha)}\text{-}5]$ in water is shown as Figure S3 (Supporting Information). The molecular ion, $M^+ = 1101$ *m*/*e*, and the intact ions, M^{2+} and M^{3+}, 601 *m*/*e* and 380 *m*/*e*, respectively, are readily observed. The FAB and ESI mass spectral data on $[15\text{-}MC_{Cu(II)N(picha)}\text{-}5]$ are consistent with the conclusion that these metallacrowns retain their structure in solution (MeOH, water, and DMF) when complexed to the lanthanide ions (Ln = La(III), Nd(III), Sm(III), Eu(III), Gd(lll), Dy(III), Ho(III), Er(III), and Yb(III)).

The solution speciation of the amino hydroximate metallacrowns were studied in methanol by FAB-MS^+ or ESI-MS^+ or in water by ESI-MS^+. All of the aminohydroximate complexes that were studied show intact ions (M^{2+} and M^{3+}) and molecular ions (M^+) as discussed previously.[15] In particular, an ESI-MS^+ of $Gd(NO_3)_3[15\text{-}MC_{Cu(II)N(glyha)}\text{-}5]$ in water gave peaks at 305.5 *m*/*e*, 487.2 *m*/*e*, and 1033 *m*/*e* that correspond to $\{Gd[15\text{-}MC_{Cu(II)N(glyha)}\text{-}5]\}^{3+}$, $\{Gd(NO_3)[15\text{-}MC_{Cu(II)N(glyha)}\text{-}5]\}^{2+}$, and $\{Gd(NO_3)_2[15\text{-}MC_{Cu(II)N(glyha)}\text{-}5]\}^+$, respectively. The ESI-$MS^+$ spectrum of $Gd(NO_3)_3[15\text{-}MC_{Cu(II)N(glyha)}\text{-}5]$ in water is shown as Figure S4 (Supporting Information). A FAB-MS^+ spectrum

of $Gd(NO_3)_3$[15-$MC_{Cu(II)N(glyha)}$-5] in methanol reveals peaks at 1319 *m*/*e*, 1256 *m*/*e*, and 628 *m*/*e* that are consistent with a metallacrown with two nitrates and one nitrate associated, respectively. The observation of molecular ions for all of the 15-metallacrown-5 complexes indicates that these metallacrowns retain their structure when dissolved in methanol or water.

UV/Vis and CD Titrations. The formation of two of the metallacrowns was studied by UV/vis spectroscopy. A solution of $Gd(NO_3)_3$ in DMF was titrated into a solution of equal amounts of $Cu(OAc)_2$ and H_2picha in DMF. The plot of the ratio of concentrations of Gd(III) to Cu(II) versus the extinction coefficient per Cu(II) at 600 nm is shown as Figure S5 (Supporting Information). The absorbance at 600 nm decreases with addition of $Gd(NO_3)_3$ until the addition of 0.2 equiv. This behavior is expected for metallacrown formation since 0.2 equiv of Gd(III) ion is necessary to achieve a ratio of one lanthanide for every five copper(II) ions. The ligand-field band blue shifted with the addition of lanthanide(III) ion by ~8 nm. It is likely that formation of the metallacrown is facilitated by templating around the Gd(III) ion. A templating reaction would not involve a simple conversion of one species to another and may explain the lack of isosbestic conversion to product. The extinction coefficient of the Cu(II) ligand-field band observed at a lanthanide-to-copper ratio of 1:5 was consistent with an authentic sample of $Gd(NO_3)_3$[15-$MC_{Cu(II)N(picha)}$-5] dissolved in DMF ($\lambda_{max} = 600$ nm, $\epsilon = 96\ M^{-1}\ cm^1$ per Cu(II)). This observation would indicate that an intact metallacrown structure is present in DMF (a conclusion that is supported by the FAB-MS spectrum). With the further addition of 0.2−1 equiv of lanthanide there is no change in the copper(II) ligand-field band, indicating that the presence of excess lanthanide ion does not disturb the metallacrown structure.

We previously reported[15] the CD spectra for the resolved Nd-$(NO_3)_3$[15-$MC_{Cu(II)N(L-alaHA)}$-5]. One can use these CD spectral bands to monitor the stability, ligand exchange dynamics, and competition of metallacrowns between other ligands. An approximately 1 mM solution of the $Nd(NO_3)_3$[15-$MC_{Cu(II)N(L-alaHA)}$-5] dissolved in either water or HEPES-buffered pH 7.0 solution did not show evidence of decomposition for 331 h (=14 days). Addition of acid to give a pH of 2.14 led to immediate loss of the CD spectrum consistent with decomposition of the metallacrown.

Such behavior was not observed above pH 6. The addition of 5 equiv of D-alaha to $Nd(NO_3)_3$[15-$MC_{Cu(II)N(L-alaha)}$-5] in pH 7.0 solution led to an immediate decrease in signal intensity at 630 nm (the maximal negative intensity for the L-isomer) and a small increased (positive) $\Delta\epsilon$ at 545 nm. These peaks continued to decrease for several hours, and after 10 h all CD intensity was lost. These data are consistent with decomposition of the metallacrown into the $Cu^{II}(alaha)_2$ complex which was prepared independently. Addition of 1 equiv of Na_2EDTA in pH 7.0 solution led to a 15% decrease in the signal for Nd-$(NO_3)_3$[15-$MC_{Cu(II)N(L-alaha)}$-5]. Subsequent additions of 1 equiv each led to further diminution (but no spectral shift) of the signal until a total of 6 equiv of Na_2EDTA had been added. These data indicate that Na_2EDTA causes decomposition of the metallacrown; however, all six ions of a single metallacrown are removed by EDTA before a second equivalent of metallacrown is destroyed. Addition of human serum transferrin does not cause a change in the CD spectrum of the metallacrown.

NMR Investigations. The solution speciation of the 15-metallacrown-5 structures was studied using ^{1}H NMR of the paramagnetically shifted resonances of the ligand protons. The ^{1}H NMR resonances of all of the metallacrowns formed with H_2picha and copper(II) as ring metal are presented in Table S1.[44] A spectrum of $La(NO_3)_3$[15-$MC_{Cu(II)N(picha)}$-5] in DMSO-d_6 is shown as Figure S7 (Supporting Information) and is representative of all of the $Ln(NO_3)_3$[15-$MC_{Cu(II)N(picha)}$-5] structures. All of these metallacrowns have four distinct resonances that are paramagnetically shifted: one proton resonance at approximately 11 ppm, two at ≈35 ppm (this resonance sometimes appears to be a single resonance due to broad line widths that do not allow for full resolution of the resonances) and a fourth resonance at 90 ppm that is very broad with a peak width of almost 10 ppm. Each picoline hydroximate has four chemically distinct protons. The simplicity of the spectra, in seeing only one set of ligand resonances, can be ascribed to the five-fold pseudosymmetry of the molecule. Other ^{1}H NMR studies of metallacrowns have shown that the presence of resonances due to the ligand is consistent with one species in solution.[45] Thus, while the peaks in the NMR spectra have not been unambiguously assigned, the simplicity of the spectra suggests that the four resonances are due to the four ligand protons.[43]

The NMR spectra of $Eu(NO_3)_3$[15-$MC_{Cu(II)N(picha)}$-5] and Nd-$(NO_3)_3$[15-$MC_{Cu(II)N(picha)}$-5] in methanol were taken immediately and after 3 days. Both NMR spectra were identical, indicating that the solution had not changed composition during this period. In these spectra no free ligand resonances were found in the diamagnetic region. A freshly prepared sample of $Gd(NO_3)_3$-[15-$MC_{Cu(II)N(picha)}$-5] in water and the same sample in solution for 5 days had identical NMR spectra. When 15 equiv of nitric acid is added (pH = 3), the solution bleaches and the ligand proton resonances are shifted to the diamagnetic region. In contrast, the metallacrowns are stable for days at pH = 6−10.

The NMR spectrum of $Eu(NO_3)_3$[15-$MC_{Cu(II)N(glyha)}$-5] in methanol-d_4 is shown as Figure S6 (Supporting Information). With glycine hydroxamic acid, it is theoretically possible to observe two proton resonances for the two α protons; however, we observe only one broad resonance. In Figure S6, the peak at 15.85 ppm is an impurity and the peaks at 7.9, 4.8, and 3.3 ppm can be assigned to residual solvent proton resonances. The proton resonance that is paramagnetically shifted to approximately 35 ppm is assigned to the α protons of glycine hydroximate.

Relaxivity of 15-Metallacrown-5 Structures with Gd(III). Proton relaxation enhancement studies of the gadolinium 15-metallacrown-5 structures were undertaken. The proton relaxation rate of **1** was measured at different concentrations in water at 20 °C and 30 MHz. A plot of the relaxation rate (s^{-1}) versus concentration (mM) is shown as Figure 5. The slope of the fit line is the relaxivity of the complex while the *y*-intercept is the diamagnetic contribution to the relaxivity by water.[25]

The relaxivity of **1** (9.8 $mM^{-1}\ s^{-1}$) is significantly higher than the relaxivity of $[Gd(DTPA)]^{2-}$, a currently used MRI

(40) Colton, R.; Tedesco, V.; Traeger, J. C. *Inorg. Chem.* **1992**, *31*, 3865.
(41) Colton, R.; James, B. D.; Potter, 1. D.; Traeger, J. C. *Inorg. Chem.* **1993**, *32*, 2626.
(42) ^{1}H NMR spectra of $Gd(NO_3)_3$[15-$MC_{Ni(II)N(picha)}$-15], **9** and $Nd(NO_3)_3$-[15-$MC_{Ni(II)N(picha)}$-15], **10**, were taken in methanol, but the spectra showed completely unresolved peaks ranging from 60 to 0 ppm.
(43) Previous studies[7] on [12-$MC_{Mn(III)N(shi)}$-4], where shi has four chemically distinct protons, have shown the presence of four resonances in the NMR spectrum. In these studies, [12- $MC_{Mn(III)N(shi)}$-4] was synthesized with selectively deuterated ligands and it was proved that the set of four resonances in the NMR spectrum of [12-$MC_{Mn(III)N(shi)}$-4] was due to one metallacrown species with a fourfold symmetry of the molecule.
(44) Franczyk, T. S.; Czerwinski, K. R.; Raymond, K. N. *J. Am. Chem. Soc.* **1992**, *114*, 8138.
(45) Weber, E.; Toner, J. L.; Goldberg, I.; Vogtle, F.; Laidler, D. A.; Stoddart, J. F.; Bartsch, R. A.; Liotta, C. L. *Crown Ethers and Analogs*; John Wiley and Sons: New York, 1989.

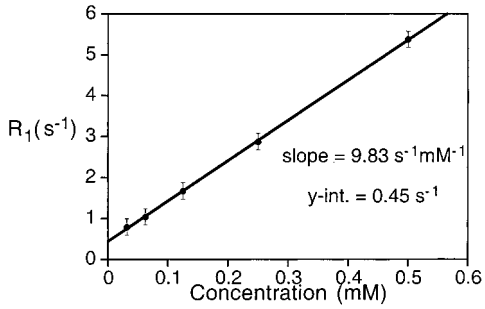

Figure 5. Determination of the relaxivity of $Gd(NO_3)_3$[15-$MC_{Cu(II)N(picha)}$-5] in water.

Table 4. Comparison of the Relaxivity of Several Complexes

complex	R_1, s^{-1} mM^{-1}	temp, °C	freq, MHz
$Gd(NO_3)_3$[15-$MC_{Cu(II)N(picha)}$-5]	9.8	20	30
$Gd(NO_3)_3$[15-$MC_{Cu(II)N(L-glyha)}$-5]	4.9	20	30
$La(NO_3)_3$[15-$MC_{Cu(II)N(picha)}$-5]	0.94	20	30
$[Gd(DTPA)]^{2-}$ [a]	4.8	25	20
$[Gd(DTPA)]^{2-}$ [a]	3.7	37	20
$[Gd(DOTA)]^{-}$ [a]	4.7	25	20
$[Gd(DOTA)]^{-}$ [a]	3.4	37	20
$[Gd(DOTA)]^{-}$ [a]	7.2	23	10
Gd(aqua ion)[a]	9.1	35	20
Cu(aqua ion)[a]	0.81	35	20
$Cu(Me_4[14]aneN_4)$[a]	0.14	37	20

[a] Values obtained from ref 25.

contrast agent that has a relaxivity of 4.8 mM^{-1} s^{-1} (25 °C and 30 MHz).[25] Some variations occur in the relaxivity if the temperature and frequency are altered, so only a qualitative comparison can be made. Lower relaxation rates occur at higher temperature, and higher rates occur at lower frequency, as shown in Table 4 for $Gd(DOTA)^-$ and $[Gd(DTPA)]^{2-}$. A relaxivity of 9.8 mM^{-1} s^{-1} is significantly higher than the rates for these two complexes, and **1** would probably still be a more efficient water proton relaxing agent at 25 °C and 30 MHz. The water relaxation rates for other metallacrowns are provided in Table 4.

Magnetism. The variable-temperature magnetic susceptibility of several 15-metallacrown-5 structures was measured from 4 to 300 K, and the results are presented in Table 5.[46] The 15-metallacrown-5 structures with Cu(II) and Ni(II) as ring metals and La(III), Nd(III), Sm(III), Eu(III), Gd(III), Dy(III), Ho(III), Er(III), and Yb(III) captured in the interior provide a wide range of magnetic moments. As can be seen in Table 5, metallacrowns with the same inorganic composition have similar magnetic moments regardless of the organic ligand used. The metallacrowns with diamagnetic ions encapsulated in the center, La(III), Ca(II), and UO_2(II), have the lowest magnetic moments. Moments as high as 10.9 μ_B can be achieved when Dy(III) and Ho(III) are encapsulated in the metallacrown ring.

The magnetic susceptibility of $La^{III}(NO_3)_3$[15-$MC_{Cu(II)N(picha)}$-5] was measured over the temperature range 2.2−300 K. The molar susceptibility and magnetic moment versus temperature are shown as Figure S8 (Supporting Information). The shape of the curve indicates that antiferromagnetic interactions are present between nearest-neighbor Cu(II) ions in the metallacrown ring. This gives the cluster an $S = {}^1/_2$ ground state at low temperatures and was verified by a saturation magnetization study of the metallacrown. A plot of the magnetization versus

(46) Sessler, J. L.; Mody, T. D.; Hemmi, G. W.; Lynch, V. *Inorg. Chem.* **1993**, *32*, 3175.

Table 5. Magnetic Moments of 15-Metallacrown-5 Complexes

Ln(III)	magnetic moment μ_B 4 K	300 K
$La(NO_3)_3$[15-$MC_{Cu(II)N(picha)}$-5]	1.83	4.06
$Ca(NO_3)_2$[15-$MC_{Cu(II)N(picha)}$-5][b]	1.94	3.85
$UO_2(NO_3)_2$[15-$MC_{Cu(II)N(picha)}$-5][b]	1.99	4.44
$Nd(NO_3)_3$[15-$MC_{Cu(II)N(picha)}$-5]	2.64	5.38
$Nd(NO_3)_3$[15-$MC_{Cu(II)N(Lalaha)}$-5][a]	2.20	5.05
$Nd(NO_3)_3$[15-$MC_{Cu(II)N(Lpheha)}$-5][a]	2.13	5.26
$Sm(NO_3)_3$[15-$MC_{Cu(II)N(picha)}$-5]	1.85	4.26
$Eu(NO_3)_3$[15-$MC_{Cu(II)N(picha)}$-5]	1.95	5.34
$Eu(NO_3)_3$[15-$MC_{Cu(II)N(iqha)}$-5]	1.75	4.89
$Eu(NO_3)_3$[15-$MC_{Cu(II)N(L-leuha)}$-5][a]	1.73	4.37
$Eu(NO_3)_3$[15-$MC_{Cu(II)N(glyha)}$-5]	1.97	6.16
$Gd(NO_3)_3$[15-$MC_{Cu(II)N(picha)}$-5]	8.45	8.98
$Gd(NO_3)_3$[15-$MC_{Cu(II)N(iqha)}$-5]	8.56	8.89
$Gd(NO_3)_3$[15-$MC_{Cu(II)NL-tyrha)}$-5][a]	7.97	8.30
$Gd(NO_3)_3$[15-$MC_{Ni(II)N(picha)}$-5]	7.79	9.09
$Dy(NO_3)_3$[15-$MC_{Cu(II)N(picha)}$-5]	10.07	10.87
$Ho(NO_3)_3$[15-$MC_{Cu(II)N(picha)}$-5]	9.18	10.94
$Er(NO_3)_3$[15-$MC_{Cu(II)N(picha)}$-5]	6.53	9.66
$Yb(NO_3)_3$[15-$MC_{Cu(II)N(picha)}$-5]	3.57	5.86

[a] Synthesis and characterization of complex described in ref 17. [b] Synthesis and characterization of complex described in ref 18.

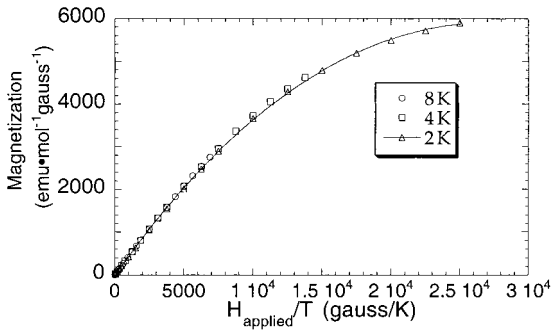

Figure 6. Magnetic data for $La^{III}(NO_3)_3$[15-$MC_{Cu(II)N(picha)}$-5]. Plot of magnetization versus applied field/temperature at 2 (triangles), 4 (squares), and 8 (circles). The fit line is the Brillouin function for $S_T = {}^1/_2$.

applied field at 2, 4, and 8 K is shown as Figure 6. A curve-fitting analysis was applied to the data using the Brillouin function for an $S_T = {}^1/_2$ spin system. This is shown as the line through the data in Figure 6.

The variable-temperature magnetic susceptibility and magnetic moments for **1**, $Gd(NO_3)_3$[15-$MC_{Cu(II)N(picha)}$-5], are plotted in Figure S9 (Supporting Information). The $Gd(NO_3)_3$[15-$MC_{Cu(II)N(picha)}$-5] metallacrown displays a slight upturn of μ_{eff} at $T < 15$ K, possibly indicative of a very small ferromagnetic exchange interaction between the $S_T = {}^1/_2$ of the Cu_5 ring and the Gd(III) ion or the presence of a small ZFS of the Gd(III) ion due to a small amount of out-of-state spin−orbit coupling mixed into the ^8S ground state of the Gd(III). Since $La^{III}(NO_3)_3$-[15-$MC_{Cu(II)N(picha)}$-5] is representative of the Cu_5 ring, a subtraction of χT from the χT data for $Gd(NO_3)_3$[15-$MC_{Cu(II)N(picha)}$-5] at every temperature should give the magnetic behavior of the Gd(III) ion by itself. The subtracted data are shown in Figure S10 (Supporting Information), and plotted as magnetic moment and susceptibility versus temperature. The fit to this subtracted data clearly shows Curie law free ion behavior for Gd(III) at higher temperatures ($T > 15$ K). The $T > 15$ K Curie law free ion behavior of the Gd(III) indicates that only a weak exchange interaction is present between the Gd(III) and the Cu_5 ring. At low temperatures there is some evidence for weak ferromagnetic exchange coupling as mentioned earlier. This

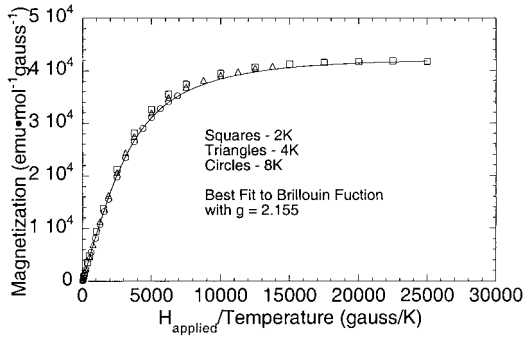

Figure 7. Plot of the saturation magnetization (magnetization vs applied field/temperature) of subtracted data at 2 (squares), 4 (triangles), and 8 K (circles). These data are fit with a Brillouin function with $S = {}^7/_2$ and $g = 2.155$.

conclusion is augmented by the plot of $Gd(NO_3)_3$[15-$MC_{Cu(II)N(picha)}$-5] variable temperature−variable field magnetization data subtracted from the $La(NO_3)_3$[15-$MC_{Cu(II)N(picha)}$-5] data shown in Figure 7. This data is plotted as a function of H/T, and the plots are superimposable at $T = 2$, 4, and 8 K and show no evidence for nesting behavior. The data are described well by the Brillouin function for $S = {}^7/_2$ shown as the fit line to the data in Figure 7.

Discussion

In this paper we exploit the strategy that we previously described to prepare an actinide specific chelating agent.[14] We utilized ligands that force five donor atoms into a plane while generating a cavity of sufficient size to accommodate a large, high-valent cation.

Salicylhydroximate was poorly suited for this application since the ligands will orient at 90° angles to one another leading to 12-metallacrown-4 structures. Instead we have chosen ligands that enforce an angle of 108° between adjacent ring metals in order to realize a planar, pentagonal ring. Picoline hydroximate, which forms two five-membered chelate rings, satisfies this requirement. Similarly, chiral and achiral amino hydroxamic acids can be employed.[15] The planar ring is obtained with copper(II) or nickel(II) as ring metals. The complexation of these transition metals into the central cavity of the 15-metallacrown-5 is strongly disfavored whereas there are many examples of the pentagonal-bipyramidal geometry for lanthanides and actinides.

The 15-metallacrown-5 molecules, listed in Table 5, demonstrate the generality of this approach. The planar 15-metallacrown-5 ring structure is able to recognize and encapsulate Ln(III), UO_2^{2+}, and Ca(II) ions.[14,15] The metal complexes were synthesized using a metal salt, $Cu(OAc)_2$ or $Ni(OAc)_2$, and a ligand, picoline hydroxamic acid (H_2picha) or the hydroxamic acid of an amino acid, with ${}^1/_5$ equiv of lanthanide nitrate to yield a metallacrown, $Ln(NO_3)_3$[15-$MC_{Cu(II)N(ligand)}$-5]. This synthetic strategy was used to synthesize several complexes in a controlled and predictable manner, including [15-$MC_{Cu(II)N(ligand)}$-5] with La(III), Nd(III), Sm(III), Eu(III), Gd(III), Ho(III), Dy(III), Er(III), and Yb(III) ions incorporated in the center of the ring.

Solid State Properties. In general, the planar 15-metallacrown-5 structures fulfill the prediction of expanded ring nuclearity with the concomitant enlargement of the cavity radius. The larger radius results in 1:1 complexes with lanthanides. The lanthanides are bound by the five oxygen atoms of the ring and generally complete their coordination sphere with solvent or bidentate nitrate ions. This type of bidentate coordination of nitrate is seen for other complexes and often accompanies lanthanide ions that are bound to ligands of five, six, or seven donors.[39,47−49]

The planar 15-MC-5 structures show some similarities and predictable differences compared to planar 12-MC-4 structures. The distances and angles to the ring copper ions are similar as shown in Tables 2 and 3. The bite distances, or Cu(ring) to Cu(ring) distances, are also similar. The cavity radius of a 15-MC-5 is larger due to the 108° angles between copper ions compared to 90° angles between the ring Cu ions of the 12-MC-4 structure.[42] The difference in cavity radius is reflected in the longer Ln−O(oxime) bond distances (by ∼0.6 Å) of encapsulated metal to oxime oxygen. These longer core metal to oxime oxygen distances are what would be expected for lanthanide oxygen distances, which are typically ∼2.5 Å.[14,15,20,21] The cavity radii of the 15-metallacrown-5 complexes increase from the nonplanar $Mn(OAc)_2$[15-$MC_{Mn(III)N(shi)}$-5] configuration, 0.77 Å,[13] to the planar $La(NO_3)_3$[15-$MC_{Cu(II)N(picha)}$-5] configuration, 1.15 Å.[49] The largest cavity radius, 1.17 Å, for **5** corresponds to the metallacrown with least deviations from planarity of the ring. This metallacrown also encapsulates the lanthanide ion, Nd(III), which has an ionic radius of 1.16 Å. The metallacrown with the smallest cavity radius is **1**, where the metallacrown ring is slightly bowed in shape due to coordination of the solvent ligand bound to one side of the ring Cu(II) ions. Upon closer inspection it becomes evident that the cavity radius can have variations in size depending on the size of the encapsulated ion and the binding of axial ligands to the metallacrown ring metals. Another structural observation is that the metallacrowns with symmetrically bound axial ligands on the Ln(III) ion, **2** and **4**, have Ln(III) ions that lie directly in the plane of the five oxygen donors of the metallacrown. Complexes **3** and **5** have Ln(III) ions that are pulled out of the plane in the direction of the most bound solvent molecules. For instance, **5** has three solvents bound on one side of the metallacrown face and one solvent bound on the other. The Nd(III) ion is 0.64 Å out of plane toward the three solvent molecules. The lanthanide texaphyrins have been shown to have out-of-plane distances that correspond to ionic radii where La(III), Gd(III), and Lu(III) are displaced 0.91, 0.60, and 0.27 Å, respectively, from the least-squares plane of the five nitrogen donors, in agreement with the lanthanide contraction.[49] This type of behavior is not observed for the metallacrowns since the displacement of ions from the five oxygen donors appears to be a combination of the number and type of solvent or anion bound and the size of the cavity radius, or the degree of contortion in the plane of the ring molecules.

The $La^{III}(NO_3)_3$[15-$MC_{Cu(II)N(picha)}$-5] metallacrown provides an opportunity to evaluate magnetic interactions solely between Cu(II) ions in this structural class because the La(III) ion is diamagnetic; therefore, any paramagnetic behavior should be due exclusively to the copper(II) ions. The *high-temperature*

(47) Archibald, S. J.; Blake, A. J.; Parsons, S.; Schroder, M.; Winpenny, R. E. P. *J. Chem. Soc., Dalton Trans.* **1997**, 173.
(48) Jones, P. L.; Amoroso, A. J.; Jeffery, J. C.; McCleverty, J. A.; Psillakis, E.; Rees, L. H.; Ward, M. D. *Inorg. Chem.* **1997**, *36*, 10.
(49) The cavity radii of the 15-metallacrown-5 structures were calculated differently from those of 12-metallacrown-4 structures since the cross distance of the hydroximate oxygen in 15-metallacrown-5 does not bisect the center of the cavity. Instead, the O(oxime)−O(oxime) distance and the angle between adjacent oxime oxygens were used to calculate cavity radii. The law of sines can be used to calculate the length of the side of any triangle using two angles and a side. One side (a) of a triangle can be calculated. The side a is the distance from O(oxime) to the center of the cavity. If the radius of an oxygen atom is subtracted from this length, then the radius of the cavity left behind is obtained.

susceptibility of $La^{III}(NO_3)_3$[15-$MC_{Cu(II)N(picha)}$-5] shows a limiting value for μ_{eff} of $\sim$ 4.2 μ_B, as predicted for five isolated Cu(II) $S = {}^1/_2$ spins. The *low-temperature* susceptibility of $La^{III}(NO_3)_3$[15-$MC_{Cu(II)N(picha)}$-5] shows a limiting value for μ_{eff} of $\sim$ 1.7 μ_B, as predicted for an $S = {}^1/_2$ spin system. The $S = {}^1/_2$ ground state description determined from the susceptibility study was confirmed by studying the saturation magnetization, indicating that the Cu(II) ions in the ring are antiferromagnetically coupled. The plot of magnetization versus applied field at 2, 4, and 8 K proves that the magnetization behavior of $La(NO_3)_3$[15-$MC_{Cu(II)N(picha)}$-5] at low temperatures displays Brillouin function behavior for an isolated $S_T = {}^1/_2$ spin system.

With an understanding of the magnetic exchange of $La^{III}(NO_3)_3$[15-$MC_{Cu(II)N(picha)}$-5], we can next describe the exchange interactions for metallacrowns containing paramagnetic Ln(III) ions. A theoretical approximation of the experimental magnetic moment of noninteracting ions can be obtained if one adds χT of one ion to the χT of the other using the theoretical moments for each ion.[30] To a first approximation, the addition of χT of the theoretical magnetic moment for an uncomplexed Ln(III) to the "control" $La^{III}(NO_3)_3$[15-$MC_{Cu(II)N(picha)}$-5] provides a good estimate of our experimental data for Ln = Nd(III), Sm(III), Dy(III), Ho(III), Er(III), and Yb(III) that is shown in Table 5. This is not surprising as magnetic exchange between Cu(II) and Ln(III) is typically weak with J values in the range of 0 ± 10 cm^{-1}, perhaps due to the ineffective f orbital overlap of the Ln(III) ions with the orbitals on the bridging ligands.[19] One exception to the simple χT approximation is seen with Eu(III). Theoretically, the magnetic moment of Eu(III) is 0 due to spin−orbit coupling, yet experimentally the Eu(III) ion has a magnetic moment of $\sim$3.5 μ_B due to low-lying paramagnetic excited states. The magnetic moment data for **2** at 4 and 300 K, shown in Table 5, also shows a population of low-lying excited states at higher temperatures in addition to the magnetic moment of the five copper(II) ions.

The magnetic data for $Gd(NO_3)_3$[15-$MC_{Cu(II)N(picha)}$-5] in Figures S9, S10, and 7 are indicative of small substate splittings and support the susceptibility conclusion of very weak exchange interaction between the $S_T = {}^1/_2$ of the Cu_5 ring and the Gd(III) ion and/or small Gd(III) ZFS. Other 15-metallacrown-5 structures with an encapsulated Gd(III) ion show similar behavior, i.e., $Gd(NO_3)_3$[15-$MC_{Cu(II)N(L-tyrha)}$-5] and $Gd(NO_3)_3$[15-$MC_{Cu(II)N(glyha)}$-5]. The generality of small ferromagnetic coupling between Gd(III) and Cu(II) ions has been observed previously in the literature. Bencini and co-workers have found that the coupling between gadolinium(III) and copper(II) is isotropic and ferromagnetic for trinuclear $GdCu_2$ linear complexes.[16,17] They also observe that ferromagnetic coupling is present irrespective of whether the gadolinium is seven- or nine-coordinate, suggesting that the coordination geometry of Gd(III) does not determine the exchange-coupling mechanism. This is consistent with the magnetic behavior of the metallacrowns since the gadolinium can be seven-, eight-, or nine-coordinate depending on the number of nitrates or solvent molecules that are bound.[14,15] Recent papers have shown unambiguously that discrete copper−Gd complexes exhibit ferromagnetic exchange interactions.[22,29]

Solution Properties. The FAB-MS^+ and ESI-MS^+, NMR investigations, and UV/vis titration studies provide direct evidence for the solution integrity of 15-$MC_{Cu(II)N(ligand)}$-5 complexes. The FAB-MS^+ spectra of all 15-$MC_{Cu(II)N(ligand)}$-5 complexes provide evidence for their stability in DMF by giving the molecular weight of the species in solution. The NMR spectra of various 15-$MC_{Cu(II)N(ligand)}$-5 complexes have similar resonances whether they are taken in DMSO or methanol; therefore, they should have solution integrity in both solvents. The ESI-MS^+ spectra of $Nd(NO_3)_3$[15-$MC_{Cu(II)N(picha)}$-5] and $Yb(NO_3)_3$[15-$MC_{Cu(II)N(picha)}$-5] in water show that these metallacrowns can be stable in water. The UV/vis titrations prove that $Gd(NO_3)_3$[15-$MC_{Cu(II)N(picha)}$-5] is intact in DMF and stable to the presence of excess lanthanide. The solution speciation studies taken collectively show that, in general, the 15-metallacrown-5 complexes are stable in DMSO, DMF, methanol, and water at neutral to basic pH values.

We have considered using metallacrowns as a new class of magnetic resonance imaging agents (MRI agents). The metallacrown structure has several potential advantages in this application compared to $[Gd(DTPA)]^{2-}$. We have already shown above that the magnetic susceptibilities of metal clusters including Cu(II) and Gd(III) ions can be enhanced compared to single-ion complexes. The 15-metallacrown-5 structure provides five oxygen atoms for coordination, while three or four other sites are possibly available for the coordination of water. The metallacrown **5** has four water molecules directly bound to Nd(III), the site that would be occupied by Gd(III). $[Gd(DTPA)]^{2-}$ and $[Gd(DOTA)]^{-}$ have only one site for the coordination of water, while complexes with two sites for water binding have a relaxation rate of 6.3 mM^{-1} s^{-1} (20 MHz and 298 K).[23] Another advantage of **1** over $[Gd(DTPA)]^{2-}$ is that it has a large planar, disklike structure that favorably affects the reorientational rate of the molecule in the solution. The reorientational rate and number of coordinating water molecules are known to have a significant effect on relaxation rate.[25,28]

Table 4 shows a comparison of the relaxivity of several gadolinium metallacrowns formed with amino hydroximates. As mentioned before, large planar structures have enhanced relaxivities, in keeping with the higher relaxivity of $Gd(NO_3)_3$[15-$MC_{Cu(II)N(L-tyrha)}$-5] of 9.43 mM^{-1} s^{-1} compared with 4.22 mM^{-1} s^{-1} for the smaller, more compact $Gd(NO_3)_3$[15-$MC_{Cu(II)N(L-alaha)}$-5]. A qualitative comparison of the relaxivity of $La(NO_3)_3$[15-$MC_{Cu(II)N(picha)}$-5]with the Cu(aqua ion) leads to the conclusion that these metallacrowns retain their integrity in water. The relaxivity of Cu(aqua ion) is 0.81 mM^{-1} s^{-1}.[25] If the metallacrown is dissociating and binding to water, the relaxivity of $La(NO_3)_3$[15-$MC_{Cu(II)N(picha)}$-5] would be equal to 5×0.81 since the concentration is per cluster and there are five copper ions per metallacrown. The relaxivity of $La(NO_3)_3$[15-$MC_{Cu(II)N(picha)}$-5] (R_1 = 0.94 mM^{-1} s^{-1}) is actually closer to the relaxivity of a 5 mM solution of copper(II) ions bound in a macrocycle ($Cu(Me_4[14]aneN_4)$, R_1 = 0.14 mM^{-1} s^{-1}), where its relaxation rate is 0.70 s^{-1}.

Of course, there are issues beyond simple relaxivities that are important in developing a useful MRI agent. In particular, one must assess the stability of the proposed agent in the presence of biological reductants or metal chelating agents. Our initial screens suggest that the present generation of metallacrowns may not withstand the thermodynamic requirements of this system. Using CD titrations, we have shown that metallacrowns alone are stable in pH 7.0 solution for $\gg$2 weeks with virtually no evidence of decomposition. We also know that these molecules do not exchange hydroximate ligands rapidly under these conditions. However, the addition of acid (to pH 2, which might be found in the stomach) leads to immediate complex decomposition. Furthermore, excess hydroxamate ligand causes decomposition of the 15-MC-5 to the bis hydroxamate species $Cu^{II}(hydroxamate)_2$. Finally, strong chelating agents such as EDTA will quantitatively remove copper and Ln(III) from the metallacrown. Interestingly, the serum iron transport protein

transferrin will not destroy the metallacrown. Undoubtedly this is due to slow kinetics of metal removal (the large metallacrown apparently cannot fit into the iron binding site to initiate metal removal) since transferrin should be thermodynamically capable of removing Cu(II) from these metallacrowns. Thus, we are now looking for more exchange inert or higher affinity complexes for the next generation of metallacrown ligands. Despite these setbacks, these metallacrowns illustrate in principle a new design strategy to both enhance the magnetic susceptibility of a molecule and simultaneously increasing the number of exchangeable Gd(III)-bound water molecules.

Acknowledgment. We thank Professor Jason Halfen for useful comments on the manuscript and Professor Robert R. Sharp for use of his NMR spectrometer to determine relaxivities of the metallacrowns. We thank the University of Michigan for the funds to support this research.

Supporting Information Available: X-ray crystallographic files, in CIF format, for three structures. Figures S1−S10 consisting of mass and NMR spectra and plots of χ_M and μ_{eff} as functions of temperature for various Cu 15-MC-5 lanthanide complexes and a plot of the titration of $Gd(NO_3)_3$ into $Cu(OAc)_2$ and H_2picha. This material is available free of charge via the Internet at http://pubs.acs.org.

IC9800233